Supplemental Material for "System Identification of *Drosophila* Olfactory Sensory Neurons"

Anmo J. Kim Aurel A. Lazar Yevgeniy B. Slutskiy*

Contents

*The names of the authors are alphabetically ordered.

1 White Noise Waveform Analysis

Reverse-correlation analysis requires using odor test stimuli with a constant spectral density. We designed odor test stimuli with an approximately flat spectrum of up to 30 Hz (Fig. S1). Since the bandwidth of Or59b OSNs is approximately 25 Hz (data not shown), reverse-correlation analysis can be applied. The autocorrelation of the odor test stimuli is shown in Figure S2.

Spike-triggered analysis requires stimuli with a Gaussian distribution. The distribution of five white noise odor waveforms with different mean concentration values (19, 27, 39, 56, 89, and 112 ppm) closely follows the Gaussian distribution (Fig. S3).

The footprint or input space of the nonlinear transformation identified with the white noise odor protocol is shown in Figure S4. The color code is associated with the 6 different mean concentration values.

2 Methods of Least Square Regression for Nonlinear blocks

We estimated the 1D nonlinearity block using two least-square regression methods: polynomial regression and Ridge regression. Ridge regression was further employed for the estimation of 2D nonlinearities.

2.1 1D Case

2.1.1 Least Squares

Let $f : X \to Y$ be a function and, for simplicity, assume that $X, Y \subseteq \Re$.

Assume that f is unknown. Known, however, are the measurements $\{y_1, y_2, \ldots, y_N\}$ of the function f at irregularly spaced points $\{x_1, x_2, \ldots, x_N\}$, i.e., $y_i = f(x_i)$, $i = 1, \ldots N$.

Our goal is to estimate the values $\{\hat{y}_1, \hat{y}_2, \ldots, \hat{y}_M\}$ of f at the regularly spaced points $\{\hat{x}_1, \hat{x}_2, \ldots, \hat{x}_M\}$. In other words, $\hat{x}_i$ are such that $\hat{x}_i - \hat{x}_{i-1} = h$, for all $i = 2, \ldots, M$ and some $h \in \Re$. One way to determine the values $\hat{y}_i$ is by using linear interpolation and least squares. Let $\mathbf{y} = [y_1, y_2, \ldots, y_N]$, $\mathbf{x} = [x_1, x_2, \ldots, x_N]$. Similarly, let $\hat{\mathbf{y}} = [\hat{y}_1, \hat{y}_2, \ldots, \hat{y}_M]$ and $\hat{\mathbf{x}} = [\hat{x}_1, \hat{x}_2, \ldots, \hat{x}_M]$.

Given $y_i = f(x_i)$ such that $\hat{x}_j \leq x_i \leq \hat{x}_{j+1}$ for some $j \in [1, \ldots, M-1]$, we can use linear interpolation to write

$$y_i = \hat{y}_j + (\hat{y}_{j+1} - \hat{y}_j)\theta_i = (1 - \theta_i)\hat{y}_j + \theta_i \hat{y}_{j+1}, \qquad \text{where} \qquad \theta_i = \frac{x_i - \hat{x}_j}{\hat{x}_{j+1} - \hat{x}_j}.$$

If the problem is well posed, then each y_i is a linear combination of $\hat{y}_j$'s and we can write

$$\mathbf{y} = \mathbf{A}\hat{\mathbf{y}} + \varepsilon,$$

where $\mathbf{A}$ is the interpolation matrix and $\varepsilon \in \Re^N$ is the residual.

To find the optimal $\hat{y}$, we solve the following unconstrained minimization problem:

$$\min_{\hat{\mathbf{y}}} \quad \|\varepsilon\|_2^2 \qquad \Longleftrightarrow \qquad \min_{\hat{\mathbf{y}}} \quad \|\mathbf{y} - \mathbf{A}\hat{\mathbf{y}}\|_2^2.$$

The problem above is convex since the objective function is quadratic in $\hat{\mathbf{y}}$. We can find the optimal solution $\hat{\mathbf{y}}^*$ by setting the gradient of the objective function to zero. We thus obtain the normal equation

$$\mathbf{A}^T\mathbf{A}\hat{\mathbf{y}} - \mathbf{A}^T\mathbf{y} = 0.$$

The optimal solution $\hat{\mathbf{y}}^*$ is given by

$$\hat{\mathbf{y}}^* = (\mathbf{A}^T\mathbf{A})^{-1}\mathbf{A}^T\mathbf{y}.$$

We note that the solution exists and is unique if the columns of $\mathbf{A}$ are independent.

For the case when the problem is ill-posed we have to use a different method.

2.1.2 Tikhonov Regularization

If the problem is ill-posed, we can introduce a regularization parameter to the objective function and attempt to solve the Tikhonov regularization problem:

$$\min_{\hat{\mathbf{y}}} \quad \|\mathbf{y} - \mathbf{A}\hat{\mathbf{y}}\|_2^2 + \delta\|\hat{\mathbf{y}}\|_2^2, \quad \text{where} \quad \delta \in \Re_{[0,\infty]}$$

The problem is clearly convex. The normal equation is given by

$$(\mathbf{A}^T\mathbf{A} + \delta I)\hat{\mathbf{y}} = \mathbf{A}^T\mathbf{y}$$

and the optimal analytical solution is

$$\hat{\mathbf{y}}^* = (\mathbf{A}^T\mathbf{A} + \delta\mathbf{I})^{-1}\mathbf{A}^T\mathbf{y}.$$

We note that because $\mathbf{A}^T\mathbf{A} + \delta\mathbf{I} \succ 0$, i.e., positive definite, the Tikhonov regularized least squares requires no rank assumptions about $\mathbf{A}$.

2.1.3 Smoothing Regularization (1D Ridge Estimator)

An extension of Tiknonov regularization is the smoothing regularization. The idea is the same as before, namely to introduce a regularizer so as to convert an ill-posed problem into a tractable one.

Assuming that the function $f : X \rightarrow Y$ is smooth, instead of adding $\|\hat{\mathbf{y}}\|$, we can add a regularizer of the form $\|\mathbf{D}^i\hat{\mathbf{y}}\|$, where the matrix $\mathbf{D}^i$ represents an approximate differentiation of the ith order (typically $i = 1, 2$). This way $\|\mathbf{D}^i\hat{\mathbf{y}}\|$ represents a measure of the variation or smoothness of $\hat{\mathbf{y}}$.

We therefore solve the following convex optimization problem:

$$\min_{\hat{\mathbf{y}}} \quad \|\mathbf{y} - \mathbf{A}\hat{\mathbf{y}}\|_2^2 + \delta\|\mathbf{D}^i\hat{\mathbf{y}}\|_2^2, \quad \text{where} \quad \delta \in \Re_{[0,\infty]}.$$

The optimal solution is given by

$$\hat{\mathbf{y}}^* = \left[\mathbf{A}^T\mathbf{A} + \delta(\mathbf{D}^i)^T\mathbf{D}^i\right]^{-1} \mathbf{A}^T\mathbf{y}.$$

The operator $\mathbf{D}^i$ is easy to postulate in matrix form. For example, given some $\hat{y}_i$, the first order differentiation near $\hat{y}_i$ can be approximated by

$$\frac{\hat{y}_{i+1} - \hat{y}_i}{\hat{x}_{i+1} - \hat{x}_i} \equiv \frac{\hat{y}_{i+1} - \hat{y}_i}{h},$$

since $\hat{y}_i$ are the regularly spaced points with $\hat{x}_{i+1} - \hat{x}_i = h$, $\forall i$. Thus the operator $\mathbf{D}^1$ is of the form

$$\mathbf{D}^1 = \frac{1}{h}\begin{bmatrix} -1 & 1 & 0 & \cdots & 0 & 0 & 0 \\ 0 & -1 & 1 & \cdots & 0 & 0 & 0 \\ 0 & 0 & -1 & \cdots & 0 & 0 & 0 \\ \vdots & \vdots & \vdots & & \vdots & \vdots & \vdots \\ 0 & 0 & 0 & \cdots & 1 & 0 & 0 \\ 0 & 0 & 0 & \cdots & -1 & 1 & 0 \\ 0 & 0 & 0 & \cdots & 0 & -1 & 1 \end{bmatrix} \in \Re^{(M-1)\times M}.$$

Similarly, the second order differentiation can be approximated by

$$\frac{(\hat{y}_{i+2} - \hat{y}_{i+1}) - (\hat{y}_{i+1} - \hat{y}_i)}{h^2} = \frac{\hat{y}_i - 2\hat{y}_{i+1} + \hat{y}_{i+2}}{h^2}.$$

Thus the operator $\mathbf{D}^2$ is of the form

$$\mathbf{D}^2 = \frac{1}{h^2}\begin{bmatrix} 1 & -2 & 1 & 0 & \cdots & 0 & 0 & 0 & 0 \\ 0 & 1 & -2 & 1 & \cdots & 0 & 0 & 0 & 0 \\ 0 & 0 & 1 & & 2\cdots & 0 & 0 & 0 & 0 \\ \vdots & \vdots & \vdots & \vdots & & \vdots & \vdots & \vdots & \vdots \\ 0 & 0 & 0 & 0 & \cdots & -2 & 1 & 0 & 0 \\ 0 & 0 & 0 & 0 & \cdots & 1 & -2 & 1 & 0 \\ 0 & 0 & 0 & 0 & \cdots & 0 & 1 & -2 & 1 \end{bmatrix} \in \Re^{(M-2)\times M}.$$

We note that $\|\mathbf{D}^2\hat{\mathbf{y}}\|_2^2$ represents a measure of the mean-square curvature of the underlying function $f : X \to Y$.

2.2 2D Ridge Estimator

The 2D ridge estimator essentially solves the 2-dimensional version of the smoothing regularization. Either $\|\mathbf{D}^1\hat{\mathbf{y}}\|$ or $\|\mathbf{D}^2\hat{\mathbf{y}}\|$ can be used as regularizers.

The interpolation matrix $\mathbf{A}$ can be computed by using either (1) nearest neighbor interpolation, (2) triangle (linear) interpolation or (3) bilinear (tensor product linear) interpolation.

2.3 Ridge Estimator Implementation

The ridge estimator used in this study is called gridfit and was adapted from DErrico (2005).

2.4 First Order Polynomial Regression

The first order polynomial regression finds the optimal polynomial coefficients $\hat{\alpha}$ and $\hat{\beta}$ of the nonlinearity f by minimizing the mean-squared error of the model prediction:

$$(\hat{\alpha}, \hat{\beta}) = \arg\min_{\alpha,\beta} \int_{\Re} \left(\lambda(s) - [\alpha \cdot (h * u)(s) + \beta]\right)^2 ds.$$

We note that $\hat{\alpha}$ and $\hat{\beta}$ can be obtained using the least squares estimation based on the QR decomposition.

3 Identification Using the Triangle Odor Waveforms

In order to estimate the nonlinear block in the triangle odor protocol we assumed that the linear filters are those of the white noise odor protocol. The block diagram of the LN cascade as well as the details of the identified blocks is shown in Figure S7.

References

D'Errico, J (2005) Surface Fitting using gridfit (http://www.mathworks.com/matlabcentral/fileexchange/8998), MATLAB Central File Exchange. Retrieved May 18, 2006.

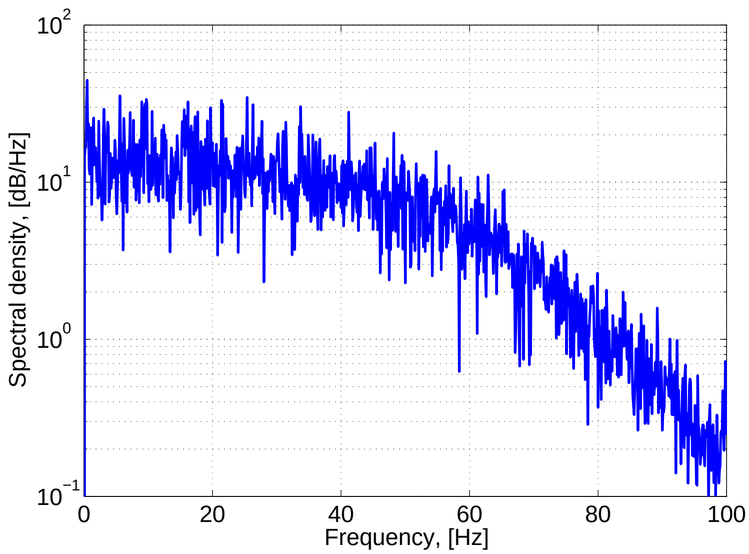

Fig. S1: The spectrum of odor test stimuli is white up to about 30 Hz.

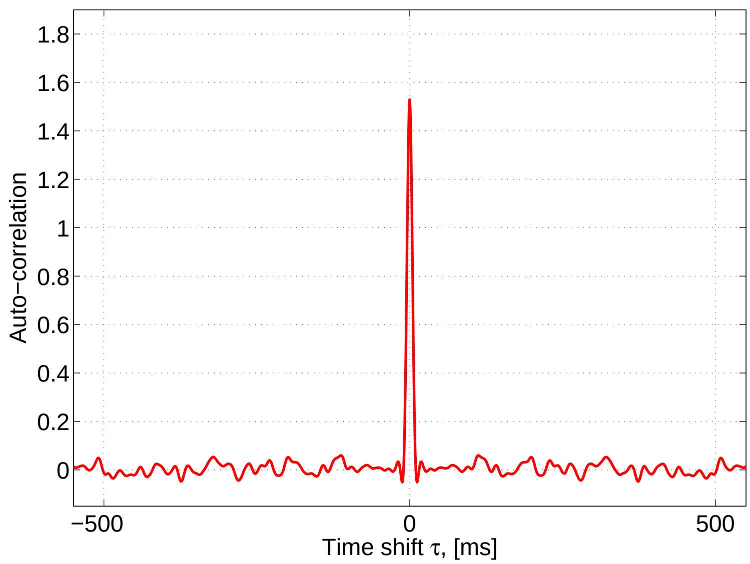

Fig. S2: Autocorrelation of the odor test stimuli.

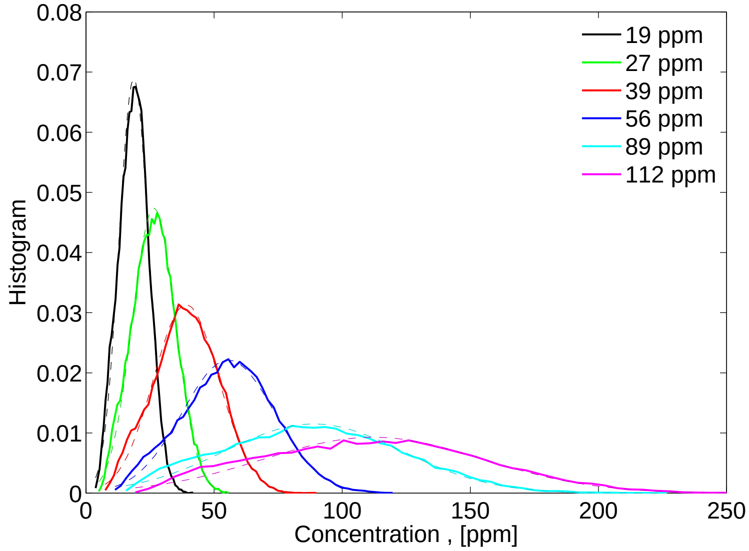

Fig. S3: The distribution of the measured white noise odor stimuli. Solid lines are histograms of odor waveforms and the dashed lines (same color) closely approximate the Gaussian distribution.

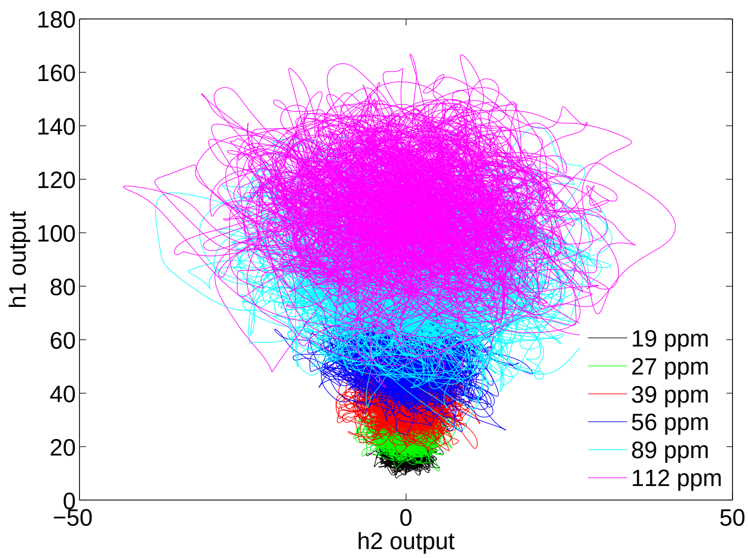

Fig. S4: Footprint of the white noise protocol

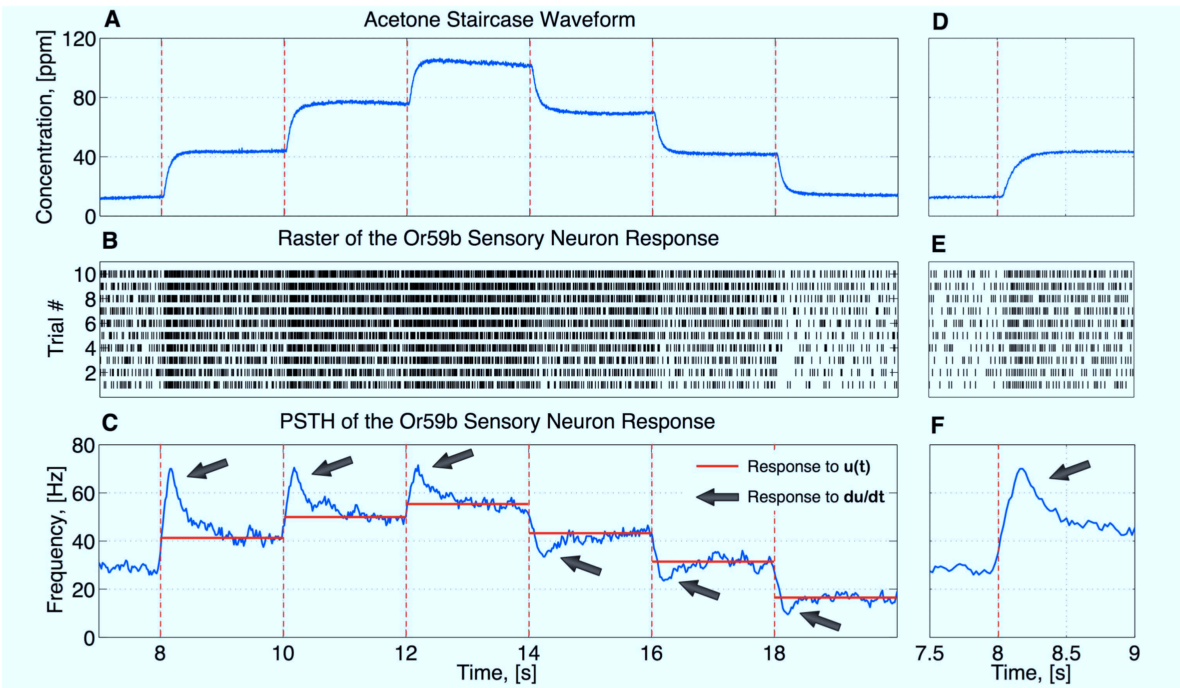

Fig. S 5: **The OSN response to the staircase waveform.** **(A)** The staircase acetone odor waveform is plotted against time. The dashed vertical lines (red) indicate the times at which the odor concentration is either increased or decreased in a step-like fashion. The length of each step is 2 s. **(B)** The raster of the OSN response to 10 consecutive presentations of the staircase odor waveform. **(C)** The PSTH of the OSN response to the staircase waveform was computed using a 100 ms bin size with a 25 ms sampling interval. Red horizontal lines denote the OSN response to the odor concentration and black arrows point out the neural response to the rate of change of the odor concentration. **(D)-(F)** A one-second-long window from (A)-(C).

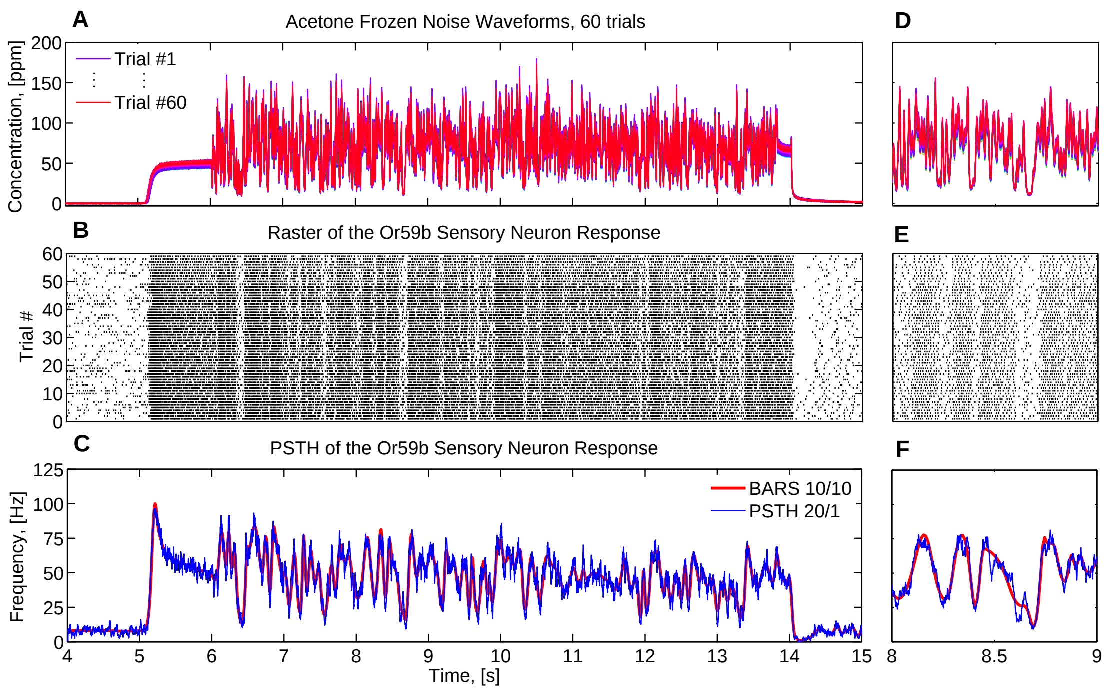

Fig. S6: **The OSN response to the acetone frozen noise odor waveform. (A)** 60 consecutive presentations of the frozen noise odor waveform. Note the remarkable reproducibility in odor delivery. **(B)** The corresponding raster of the OSN response. **(C)** The PSTH of the OSN response to the frozen noise waveform was computed using a 20 ms bin size and a 1 ms sampling interval. The BARS algorithm applied to a PSTH with non-overlapping 10 ms bins provides an additional estimate of the neural response. **(D)-(F)** A one-second-long window from (A)-(C).

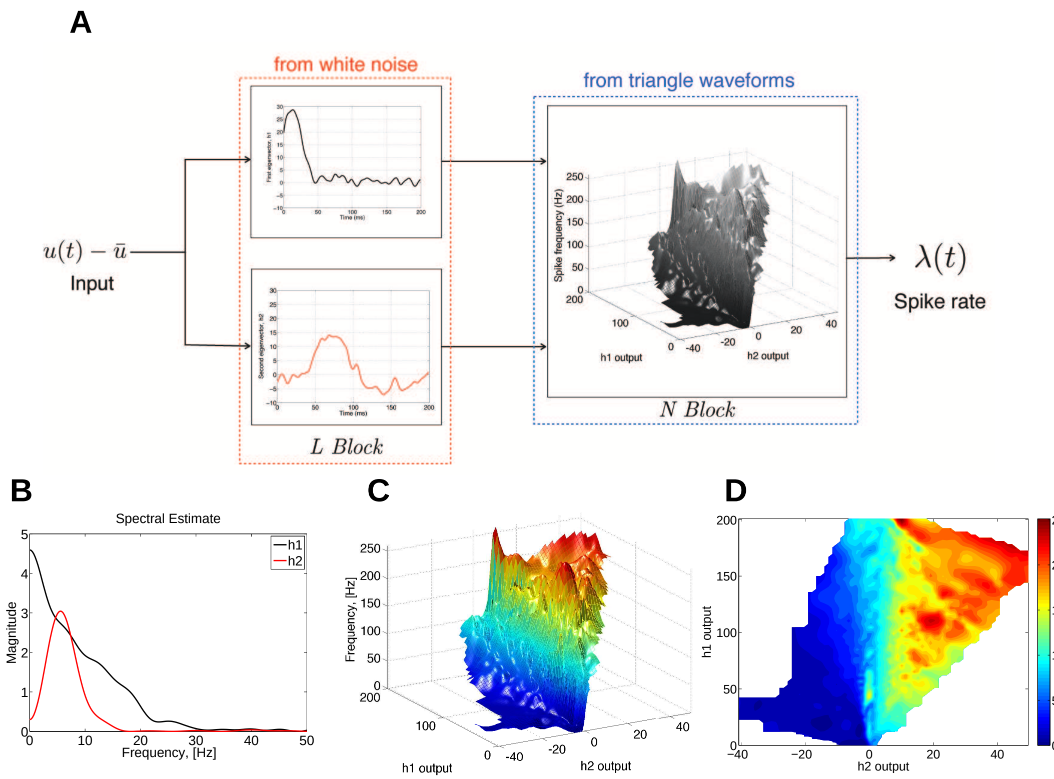

Fig. S 7: **The identification of the nonlinear block of Or59b OSNs using triangle odor waveforms (A)** The identified model of Or59b OSNs consist of two linear filters derived by using the white noise odor protocol and the two-dimensional non-linearity derived by employing the triangle odor protocol. **(B)** Two linear kernels from spike-triggered covariance analysis are used to analyze triangle waveforms. **(C)** Two-dimensional non-linearity is constructed from the input/output data obtained using the triangle odor protocol. **(D)** Contour plot of the non-linearity in (C).